

Contributions from primordial non-Gaussianity and General Relativity to the galaxy power spectrum

Rebeca Martinez-Carrillo,^a Juan Carlos Hidalgo,^b Karim A. Malik,^a Alkistis Pourtsidou^{a,c}

^aAstronomy Unit, School of Physics and Astronomy, Queen Mary University of London, Mile End Road, London, E1 4NS, United Kingdom.

^bInstituto de Ciencias Físicas, Universidad Nacional Autónoma de México, 62210, Cuernavaca, Morelos, México.

^cDepartment of Physics and Astronomy, University of the Western Cape, Cape Town 7535, South Africa

E-mail: r.martinezcarrillo@qmul.ac.uk, hidalgo@icf.unam.mx, k.malik@qmul.ac.uk, a.pourtsidou@qmul.ac.uk

Abstract. We compute the real space galaxy power spectrum, including the leading order effects of General Relativity and primordial non-Gaussianity from the f_{NL} and g_{NL} parameters. Such contributions come from the one-loop matter power spectrum terms dominant at large scales, and from the factors of the non-linear bias parameter b_{NL} (akin to the Newtonian b_{ϕ}). We use our modelling to assess the ability of Stage-IV surveys to constrain primordial non-Gaussianity. In addition, we show how this non-linear bias parameter can effectively renormalize diverging relativistic contributions at large scales.

Keywords: galaxy power spectrum, primordial non-gaussianity, relativistic cosmology

¹Corresponding author.

Contents

1	Introduction	1
2	Relativistic density contrast	2
3	Galaxy power spectrum	4
4	Results	6
4.1	Viabale bias parameter values	7
4.2	Avoiding large-scale divergences	8
5	Discussion	11

1 Introduction

In recent years our understanding of the evolution of the Universe has greatly benefited from observations. With the forthcoming Stage IV experiments such as Euclid¹ [1], the Dark Energy Spectroscopic Instrument (DESI)² [2] and the Vera C. Rubin Observatory’s Legacy Survey of Space and Time (LSST)³ [3], we are expecting to obtain high-precision measurements in order to improve our understanding of the large scale structure (LSS) of the Universe. The progress achieved over the last few years demands a comprehensive description of observables from the full theory, a general relativistic description, in order to take advantage of the detail and scales these surveys aim to map.

Most of the cosmological information is encoded in the 2-point correlation function or its Fourier space equivalent, the power spectrum, which, among other contributions, includes those of primordial non-Gaussianity (PNG). The possibility to constrain PNG through the power spectrum has been reported e.g. in Refs. [4–16], showing that the late-time statistics contain crucial information of the physics prevalent in the early universe. One of the main strategies to estimate PNG effects in the current matter distribution is to analyse the corresponding galaxy power spectrum, which is related to the underlying matter distribution through a set of bias parameters. In the past years galaxy bias has been included mostly in Newtonian descriptions of the LSS [17–21]. An extensive review, presenting some of the main studies of large scale galaxy bias can be found in Ref. [22].

The ever-increasing precision in the measurement of the power spectrum allows us to consider that, in addition to PNG contributions, general relativistic effects may also be observable at the large scales of the evolved matter distribution. This is due to the non-linear nature of the theory. Such effects in the galaxy clustering have been studied for example in Refs. [23–30].

In this paper we are interested in accounting for both relativistic and PNG effects in the galaxy distribution using a suitable parametrization of the galaxy bias. Galaxy bias in a relativistic context has been previously explored including primordial non-Gaussianities,

¹<http://euclid-ec.org>

²<https://www.desi.lbl.gov/>

³<https://www.lsst.org/>

e.g. in Refs. [31, 32], and the most suitable gauge to define the bias in, namely the comoving-synchronous gauge, has been discussed in Ref. [33].

A derivation of the local bias at second order in cosmological perturbation theory, for Gaussian and non-Gaussian initial conditions is studied in Refs. [34, 35], where it is argued that general relativistic effects affect local clustering predominantly through the distortion of the volume element of the local patch, and that modulations of the short-modes are possible only through primordial non-Gaussianity.

At one-loop order under the weak field approximation, relativistic corrections have been included for the power spectrum at intermediate scales in Ref. [36], with results extended to obtain the galaxy power spectrum using a Lagrangian bias expansion in General Relativity in Ref. [37].

More recently, methods to avoid the infrared divergences of relativistic contributions in the galaxy power spectrum, have been proposed in Refs. [38, 39].

In this paper we extend our previous work [40], by not only including relativistic corrections to the power spectrum at one-loop and the input from primordial non-Gaussianity but also introducing a bias prescription guided by the parametrization in Refs. [41, 42], and adopt a set of two parameters, a linear b_δ and a non-linear parameter b_{NL} to compute the galaxy power spectrum in the synchronous-comoving gauge⁴. We calculate the galaxy power spectrum for a range of reasonable values of the PNG and bias parameters and compare results with the forecasted measurements from Stage-IV experiments, specifically from a 15,000 deg² and a 40,000 deg² (all-sky) galaxy survey.

In addition, we show that suitable values of the bias parameters constitute an effective strategy to renormalize the (divergent) relativistic contributions at large scales without affecting the dominant PNG effect.

The paper is structured as follows: in section 2 we briefly review previous work and present the expressions for the relativistic density contrast that we used in the computation of the galaxy power spectrum. In section 3 we introduce the bias model and the mathematical expression of the galaxy power spectrum. In section 4 we present our results in a series of plots of the galaxy power spectrum with a range of values for the PNG parameters and for the non-linear bias. The spectra include the observational uncertainties from Stage-IV galaxy surveys. We also give a combination of bias parameter values which serve as an effective renormalization of the relativistic contributions, which are otherwise divergent at large scales. Finally in section 5 we discuss our results.

Throughout this paper we use the conformal time η , and denote derivatives with respect to η with a prime. Greek indices μ, ν , range from 0 to 3, lower case Latin indices, i, j , and k , range from 1 to 3.

2 Relativistic density contrast

In this section we present the basic definitions for our calculation, the expressions for the relativistic density contrast. These definitions were presented in previous works and the details of the calculation can be found in e.g. Refs. [40, 44–46]. We briefly summarise how these are obtained to facilitate the reader’s comprehension of further sections.

⁴The synchronous-comoving gauge is an adequate gauge choice to express the Lagrangian frame and the simplest to specify a galaxy bias at second order [43].

The starting point of this work is the perturbed Friedmann-Robertson-Walker line element in synchronous-comoving gauge [47, 48],

$$ds^2 = a^2(\eta)[-d\eta^2 + \gamma_{ij}dx^i dx^j], \quad (2.1)$$

where a is the scale factor and γ_{ij} the perturbed spatial metric. The matter content considered is a pressureless and irrotational fluid. The density field ρ is given by

$$\rho(\mathbf{x}, \eta) = \bar{\rho}(\eta) + \delta\rho(\mathbf{x}, \eta) = \bar{\rho}(\eta)(1 + \delta(\mathbf{x}, \eta)), \quad (2.2)$$

where $\bar{\rho}(\eta)$ is the density in the background, $\delta\rho(\mathbf{x}, \eta)$ is a small perturbation and $\delta(\mathbf{x}, \eta)$ is the density contrast.

The evolution of the density contrast $\delta(\mathbf{x}, \eta)$ is given by the continuity equation

$$\delta' + (1 + \delta)\vartheta = 0, \quad (2.3)$$

where ϑ is the trace of the deformation tensor ϑ_ν^μ , that is $\vartheta = \vartheta_\alpha^\alpha$, and the deformation tensor is defined by

$$\vartheta_\nu^\mu \equiv au^\mu_{;\nu} - \mathcal{H}\delta_\nu^\mu, \quad (2.4)$$

where u^μ is the fluid 4-velocity, \mathcal{H} the Hubble parameter in conformal time. The evolution for ϑ is given by the Raychaudhuri equation [45, 49]

$$\vartheta' + \mathcal{H}\vartheta + \vartheta_j^i \vartheta_i^j + 4\pi G a^2 \bar{\rho} \delta = 0. \quad (2.5)$$

The energy constraint is given by

$$\vartheta^2 - \vartheta_j^i \vartheta_i^j + 4\mathcal{H}\vartheta + {}^3R = 16\pi G a^2 \bar{\rho} \delta, \quad (2.6)$$

where 3R is the spatial Ricci scalar of the spatial metric γ_{ij} .

Finding a solution for the density contrast δ can be achieved by using either perturbation theory or a gradient expansion; for brevity we present the gradient approach only. In this approach the spatial part of the metric is written in terms of a conformal factor as [50, 51]

$$g_{ij} = a^2 \gamma_{ij} = a^2 e^{2\zeta} \check{\gamma}_{ij}. \quad (2.7)$$

Using this approximation, spatial gradients are small compared to time derivatives. In addition, we find that

$$\delta \sim \vartheta \sim {}^3R \sim \nabla^2. \quad (2.8)$$

This means that on large scales, the conformal metric can be approximated as $\check{\gamma}_{ij} \simeq \delta_{ij}$. The result of this simplified metric is having the Ricci scalar as a function of the curvature perturbation ζ only [44, 46]

$${}^3R = -4\nabla^2\zeta + \sum_{m=0}^{\infty} \frac{(-2)^{m+1}}{(m+1)!} [(m+1)(\nabla\zeta)^2 - 4\zeta\nabla^2\zeta] \zeta^m, \quad (2.9)$$

where ζ is expanded up to third order as

$$\zeta = \zeta^{(1)} + \frac{3}{5}f_{\text{NL}}\zeta^{(1)2} + \frac{9}{25}g_{\text{NL}}\zeta^{(1)3}, \quad (2.10)$$

with f_{NL} and g_{NL} being the usual local non-Gaussianity parameters [52].

The general solution for the density contrast in Einstein de-Sitter is of the form

$$\delta(\eta, \mathbf{x}) = C(\mathbf{x})D_+(\eta), \quad (2.11)$$

where $C(\mathbf{x})$ is given by [45]

$$C(\mathbf{x}) = \frac{{}^3R}{10\mathcal{H}_{IN}^2 D_{+IN}}, \quad (2.12)$$

where D_+ is a constant – the growth factor evaluated at some time early in the matter dominated era, denoted by subscript “ IN ”.

Using Eq. (2.9), the relativistic density contrast in Eq. (2.11) up to third order is given by

$$\delta = \delta^{(1)} + \frac{1}{2}\delta^{(2)} + \frac{1}{6}\delta^{(3)}, \quad (2.13)$$

where [40]

$$\delta^{(1)} = \frac{D_+(\eta)}{10\mathcal{H}_{IN}^2 D_{+IN}} \left(-4\nabla^2 \zeta^{(1)} \right), \quad (2.14)$$

$$\delta^{(2)} = \frac{D_+(\eta)}{10\mathcal{H}_{IN}^2 D_{+IN}} \frac{24}{5} \left[-(\nabla \zeta^{(1)})^2 \left(\frac{5}{12} + f_{\text{NL}} \right) + \zeta^{(1)} \nabla^2 \zeta^{(1)} \left(\frac{5}{3} - f_{\text{NL}} \right) \right], \quad (2.15)$$

$$\delta^{(3)} = \frac{D_+(\eta)}{10\mathcal{H}_{IN}^2 D_{+IN}} \frac{108}{25} \left[2\zeta^{(1)} (\nabla \zeta^{(1)})^2 \left(-g_{\text{NL}} + \frac{5}{9} f_{\text{NL}} + \frac{25}{54} \right) + \zeta^{(1)2} \nabla^2 \zeta^{(1)} \left(-g_{\text{NL}} + \frac{10}{3} f_{\text{NL}} - \frac{50}{27} \right) \right], \quad (2.16)$$

and the growth factor in Einstein-de Sitter is

$$D_+ = \frac{D_{+IN} \mathcal{H}_{IN}^2}{\mathcal{H}^2}, \quad (2.17)$$

with $D_{+IN} = 1$ and $\mathcal{H}_{IN} = \mathcal{H}_0$, where \mathcal{H}_0 is the conformal Hubble parameter at present time.

3 Galaxy power spectrum

To compute the galaxy power spectrum we follow the renormalized perturbative bias model of Refs. [41, 42]. This approach assumes the Taylor expansion of a general function of the density contrast, given by

$$\delta_g = c_\delta \delta + \frac{1}{2} c_{\delta^2} (\delta^2 - \sigma^2) + \frac{1}{3!} c_{\delta^3} \delta^3 + \epsilon + \mathcal{O}(\delta^4), \quad (3.1)$$

where $\sigma^2 = \langle \delta^2 \rangle$ is the variance of δ , the coefficients of the Taylor expansion c_{δ^n} constitute the bias parameters, while ϵ is a random noise variable that allows for stochasticity. This prescription was originally defined for matter density in the Eulerian frame, though we adopt

it for the Lagrangian density expressed earlier. Our parameters should thus be interpreted as Lagrangian variables⁵.

If we expand the density contrast in perturbative orders up to the leading non-linear contribution to the power spectrum, then Eq. (3.1) is expanded as

$$\delta_g = c_\delta \left(\delta^{(1)} + \frac{\delta^{(2)}}{2} + \frac{\delta^{(3)}}{6} \right) + \frac{c_{\delta^2}}{2} \left(\delta^{(1)2} + \delta^{(1)}\delta^{(2)} \right) + \dots, \quad (3.2)$$

where $\delta^{(1)}$, $\delta^{(2)}$ and $\delta^{(3)}$ are defined in Eqs. (2.14), (2.15) and (2.16) respectively.

The galaxy power spectrum is defined as

$$\langle \delta_g(k, \eta) \delta_g(k', \eta) \rangle = (2\pi)^3 P_{gg}(k, \eta) \delta_D(k + k'), \quad (3.3)$$

where k is the comoving wavenumber in Fourier space. The leading order non-linear corrections to the galaxy power spectrum are of order $\delta^{(4)}$ only. Using Eq. (3.2) and Eq. (3.3), the galaxy power spectrum $P_{gg}(k, \eta)$ is given by

$$P_{gg}(k, \eta) = (c_\delta)^2 \left[P_L(k, \eta) + 2P_R^{(1,3)}(k, \eta) + P_R^{(2,2)}(k, \eta) \right] + (2c_\delta c_{\delta^2}) [P_{R1}(k, \eta) + P_{R2}(k, \eta)], \quad (3.4)$$

where $P_L(k, \eta)$ represents the linear power spectrum, $P_R^{(1,3)}(k, \eta)$ and $P_R^{(2,2)}(k, \eta)$ are the relativistic contributions to the one-loop matter power spectrum (previously presented in Ref. [40]), and are given by

$$P_R^{(1,3)}(k, \eta) = \frac{k^3}{(2\pi)^2} P_L(k, \eta) \int_0^\infty dr P_L(kr, \eta) \left\{ 81 \left(\frac{\mathcal{H}^4}{k^4} \right) \left[\left(-g_{\text{NL}} + \frac{5}{9} f_{\text{NL}} + \frac{25}{54} \right) + \frac{1 + 2r^2}{6r^2} \left(g_{\text{NL}} - \frac{10}{3} f_{\text{NL}} + \frac{50}{27} \right) \right] \right\}, \quad (3.5)$$

$$P_R^{(2,2)}(k, \eta) = \frac{k^3}{2\pi^2} \int_0^\infty dr P_L(kr, \eta) \int_{-1}^1 dx P_L(k\sqrt{1+r^2-2rx}, \eta) \times \left\{ \left(\frac{\mathcal{H}^4}{k^4} \right) \left[\frac{6f_{\text{NL}} - 10 - 25r^2 + 25rx}{4r(1-2rx+r^2)} \right]^2 \right\}. \quad (3.6)$$

The contributions $P_{R1}(k, \eta)$ and $P_{R2}(k, \eta)$, which are not present in the one-loop matter spectrum, are given by

$$P_{R1}(k, \eta) = \frac{k^3}{(2\pi)^2} P_L(k, \eta) \int_0^\infty dr P_L(kr, \eta) \times \int_{-1}^1 dx \left(\frac{\mathcal{H}^2}{k^2} \right) \left[3f_{\text{NL}}(1+r^2+2rx) + \frac{5}{6}(3rx-6+6r^2) \right], \quad (3.7)$$

$$P_{R2}(k, \eta) = \frac{k^3}{(2\pi)^2} \int_0^\infty dr P_L(kr, \eta) \int_{-1}^1 dx P_L(k\sqrt{1+r^2-2rx}, \eta) \times \left(\frac{\mathcal{H}^2}{k^2} \right) \left[\frac{6f_{\text{NL}} - 10 - 25r^2 + 25rx}{4(1-2rx+r^2)} \right]. \quad (3.8)$$

⁵The Lagrangian bias parameters should coincide with the Eulerian set at large scales, because the coordinate change to the Eulerian frame alters quantities at small scales only [43, 45].

We now re-express the bias factors in terms of the linear and non-linear bias parameters for $P_{gg}(k, \eta)$ in terms of the c_δ and c_{δ^2} . At leading order the correspondence is straightforward and is reduced to parameters

$$b_\delta = c_\delta, \quad b_{\text{NL}} = 2c_{\delta^2}, \quad (3.9)$$

and we get

$$P_{gg}(k, \eta) = (b_\delta)^2 \left(P_L(k, \eta) + 2P_R^{(1,3)}(k, \eta) + P_R^{(2,2)}(k, \eta) \right) + (b_\delta b_{\text{NL}}) \left(P_{R1}(k, \eta) + P_{R2}(k, \eta) \right). \quad (3.10)$$

The bias parameter b_{NL} corresponds to b_ϕ introduced in Ref. [42], the latter accounts for the dominant contributions from primordial non-Gaussianity. We use a different label to emphasise that b_{NL} includes PNG as well as relativistic terms. Note, that the terms multiplied by b_{NL} include those of the *scale-dependent bias*, which is the focus of previous studies (see e.g. Refs. [17, 33]).

As can be seen from Eq. (3.10), with the parametrization chosen above, the one-loop matter power spectrum is included in the terms multiplied by the square of the linear bias, $(b_\delta)^2$. This is consistent with the fact that the relativistic solutions are part of the linear correspondence between matter density and spatial curvature (the lowest order solution in the gradient expansion). This characteristic feature of General Relativity and PNG plays a crucial role in the bias parameter fitting as we will see below.

4 Results

In this section we present the galaxy power spectrum for a set of values of interest of the galaxy bias parameters. This is best appreciated in plots of the galaxy power spectrum itself. All our calculations were performed numerically in Python, using as an input a linear power spectrum generated with the CLASS Boltzmann solver [53, 54], for realisations of the Λ CDM cosmology, taking parameter values from the Planck collaboration results [55].

In all our plots of the galaxy power spectrum, the value for the linear bias parameter is fixed to $b_\delta = 1.41$ in a survey bin with mean redshift $z = 1$, following the parametrisation [56]

$$b_\delta = \sqrt{1+z}. \quad (4.1)$$

First, we show that there is no divergence of the non-linear contributions at small scales. We plot in Fig. 1 the galaxy power spectrum of Eq. (3.10) at $z = 1$. This includes the non-Gaussianity contributions with the limiting values of parameters f_{NL} and g_{NL} reported by the Planck collaboration [57] (the value of b_{NL} for this figure is arbitrary within the perturbative expansion hierarchy).

Let us stress at this point, a technical but important issue, relevant for all plots in this paper. We show throughout the minimum value of $f_{\text{NL}} = -1$, since smaller values yield dominant (negative) contributions to the matter power spectrum on large scales. In that sense, in the non-linear contributions to the matter power spectrum we discarded the possibility of using values of $g_{\text{NL}} > 7$ [40]. We note, however, that such a restriction is not necessary in the galaxy power spectrum in general. This is because the two new contributions $P_{R1}(k, \eta)$ and $P_{R2}(k, \eta)$, balance the original one-loop terms as dictated by the values of the b_{NL} parameter as exemplified below.

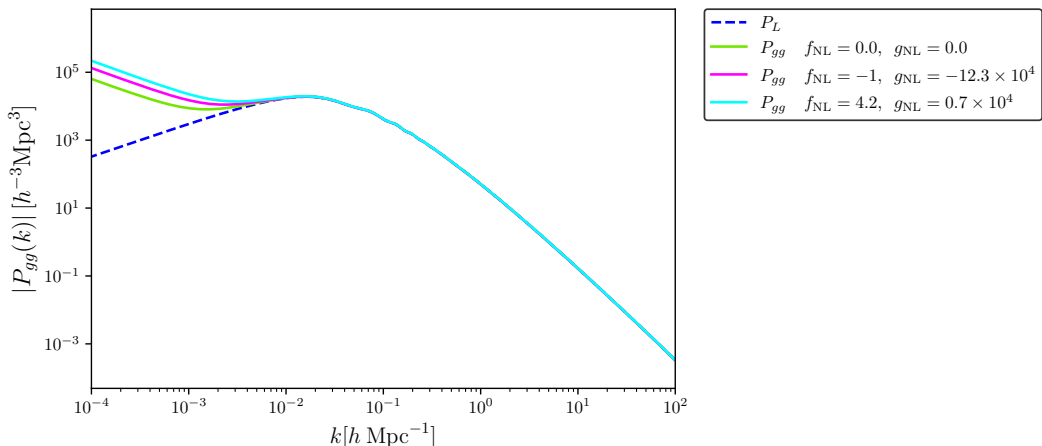


Figure 1: Galaxy power spectrum in a wide scale range, at redshift $z = 1$, $b_\delta = 1.41$ and $b_{\text{NL}} = 0.2$, for different limiting values of f_{NL} and g_{NL} reported by Planck [57]. No divergence is observed in any of the cases at small scales (large k -modes). The divergences at the other end are discussed in section 4.2.

In Fig. 2 we plot separately the contributions to the galaxy power spectrum by each term in Eq. (3.10) (setting both bias parameters to unity). The dominant contribution at large scales comes from $P_{R1}(k, \eta)$, an additional term to the one-loop matter spectrum, followed by $P_R^{(1,3)}(k, \eta)$, which is the only term with g_{NL} dependence.

Using Eq. (4.1) for b_δ , in the rest of this section we present the galaxy power spectrum for values for b_{NL} following two criteria: First we compute values for which the spectrum deviates from the linear prescription beyond the uncertainty in current and future surveys, and thus show observable relativistic or PNG contributions, and subsequently we compute values which cancel the divergent part of the relativistic contribution at large scales, thus showing observable features at large scales only in the presence of primordial non-Gaussianity.

4.1 Viable bias parameter values

In Fig. 3 and Fig. 4 we present the galaxy spectrum at redshift $z = 1$ for combinations of the limiting values of f_{NL} and g_{NL} . In each plot we display a shaded area, corresponding to the predicted 1σ measurement errors for a survey of $15,000 \text{ deg}^2$ (Euclid-like, Fig. 3), and a survey of $40,000 \text{ deg}^2$ in Fig. 4.

Our forecasts assume idealised cosmic variance limited surveys, i.e., with negligible shot noise [58]. Other specifications are the redshift bin width $\Delta z = 1.0$ at a central redshift $z = 1$, and the largest measured scale $k_{\text{min}} \simeq 2\pi/V_{\text{bin}}^{1/3} = 0.001 h\text{Mpc}^{-1}$ for a $40,000 \text{ deg}^2$ survey and $k_{\text{min}} = 0.002 h\text{Mpc}^{-1}$ for a $15,000 \text{ deg}^2$ survey. We note that shot noise contributions and, most importantly, large scale systematic effects (see e.g. [59]) are expected to increase the error budget. We fix the value of b_{NL} to show in solid lines the minimum value required to have a galaxy power spectrum that could be distinguished in forthcoming surveys considering the forecasted 1σ measurement errors.

Additionally, we show in dashed lines the smallest b_{NL} values that result in a well behaved galaxy power spectrum. As already stated, the fiducial value for b_δ is chosen to be $b_\delta = 1.41$ at a mean redshift $z = 1$.

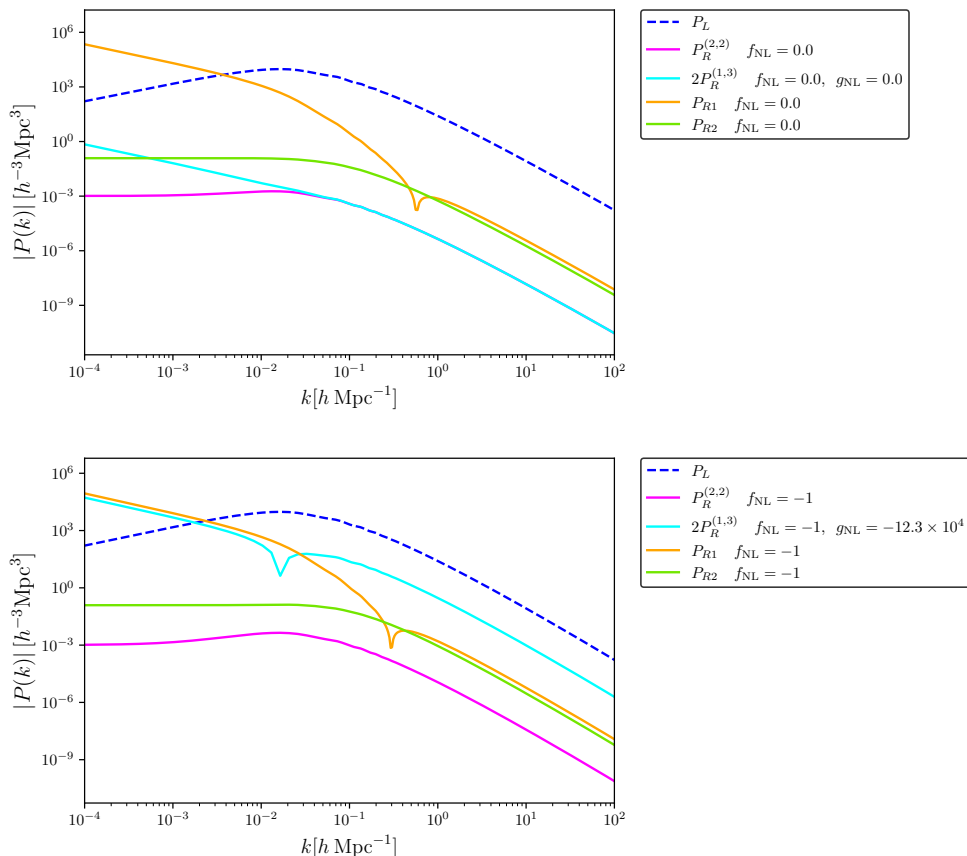


Figure 2: Contributions from each term to the galaxy power spectrum in Eq. (3.10) at redshift $z = 1$, for Gaussian initial conditions (upper plot), and for the limiting values of f_{NL} and g_{NL} reported by Planck [57] (lower plot).

4.2 Avoiding large-scale divergences

As mentioned earlier, a few recent works have argued that a divergent behaviour on large scales of the galaxy power spectrum due to the relativistic corrections is nonphysical [35, 38, 39]. In order to avoid such divergence, a coordinate transformation must be performed, which places the observed spectrum in a “local frame” where the divergences disappear.

We have found that it is possible to ease the divergences with a suitable choice of the new b_{NL} parameter. This *renormalization* method sets a parameter value which cancels the relativistic effects of the dominant terms $P_{R1}(k, \eta)$ and $P_R^{(1,3)}(k, \eta)$ at large scales, in the absence of PNG. For this bias choice, the maximum value of g_{NL} that keeps the perturbation theory hierarchy is of the order of $g_{\text{NL}} \sim 7$, since the use of higher values, even though are allowed by Planck, leads to negative contributions to the power spectrum. The result of this effective renormalization through parameter fitting is presented in Fig. 5. Note that when adding non-Gaussianity contributions the only case that departs significantly from the linear spectrum is when g_{NL} takes the minimum value allowed by Planck results.

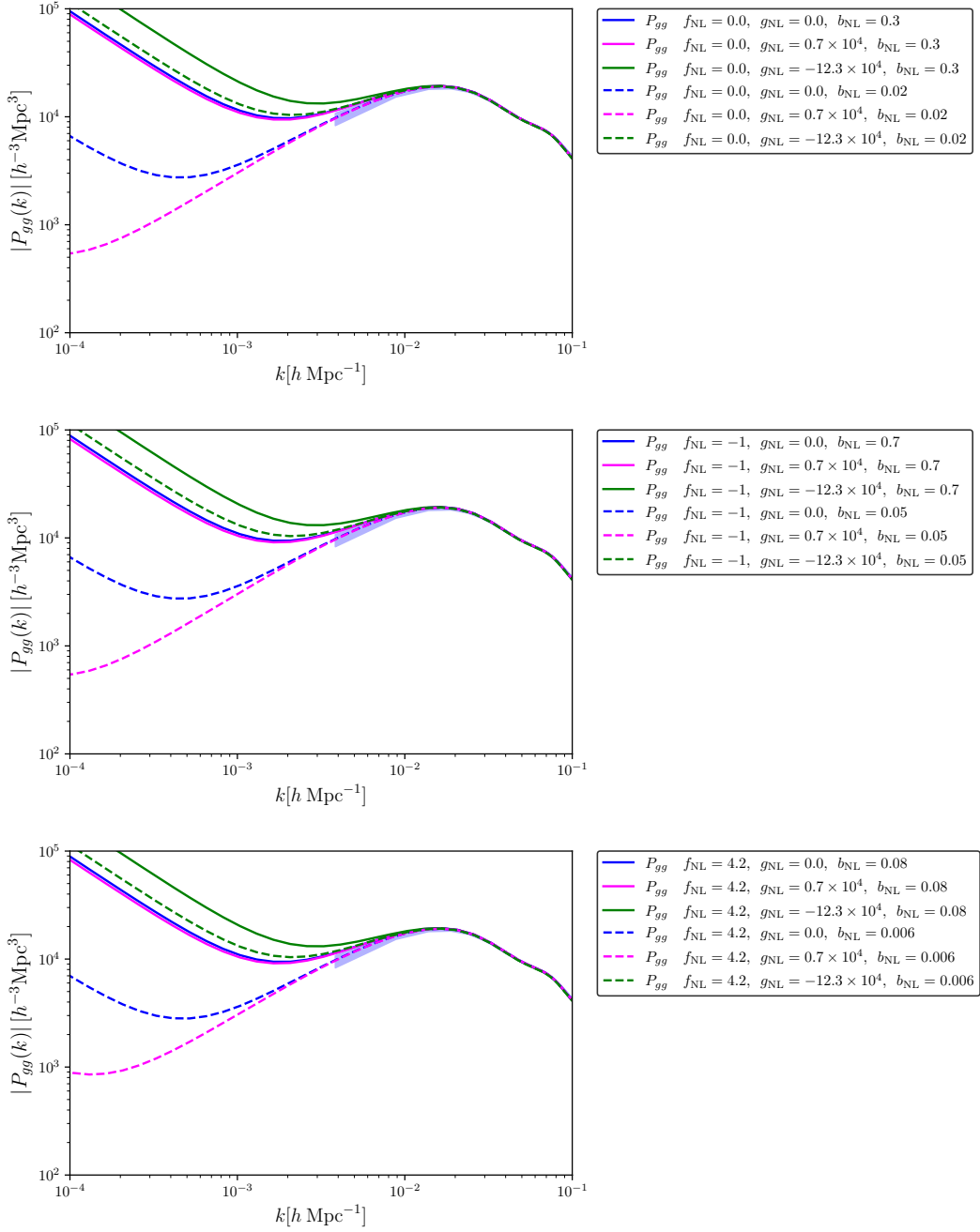


Figure 3: Galaxy power spectrum at redshift $z = 1$, with $b_\delta = 1.41$ (a choice justified in the text), for the limiting values of f_{NL} (zero for the top plot, -1 for the middle plot, and 4.2 for the bottom) each with limiting g_{NL} values reported by Planck [57]. The blue shaded area corresponds to the forecasted 1σ uncertainties of a cosmic variance limited survey of $15,000 \text{ deg}^2$. See text for more details.

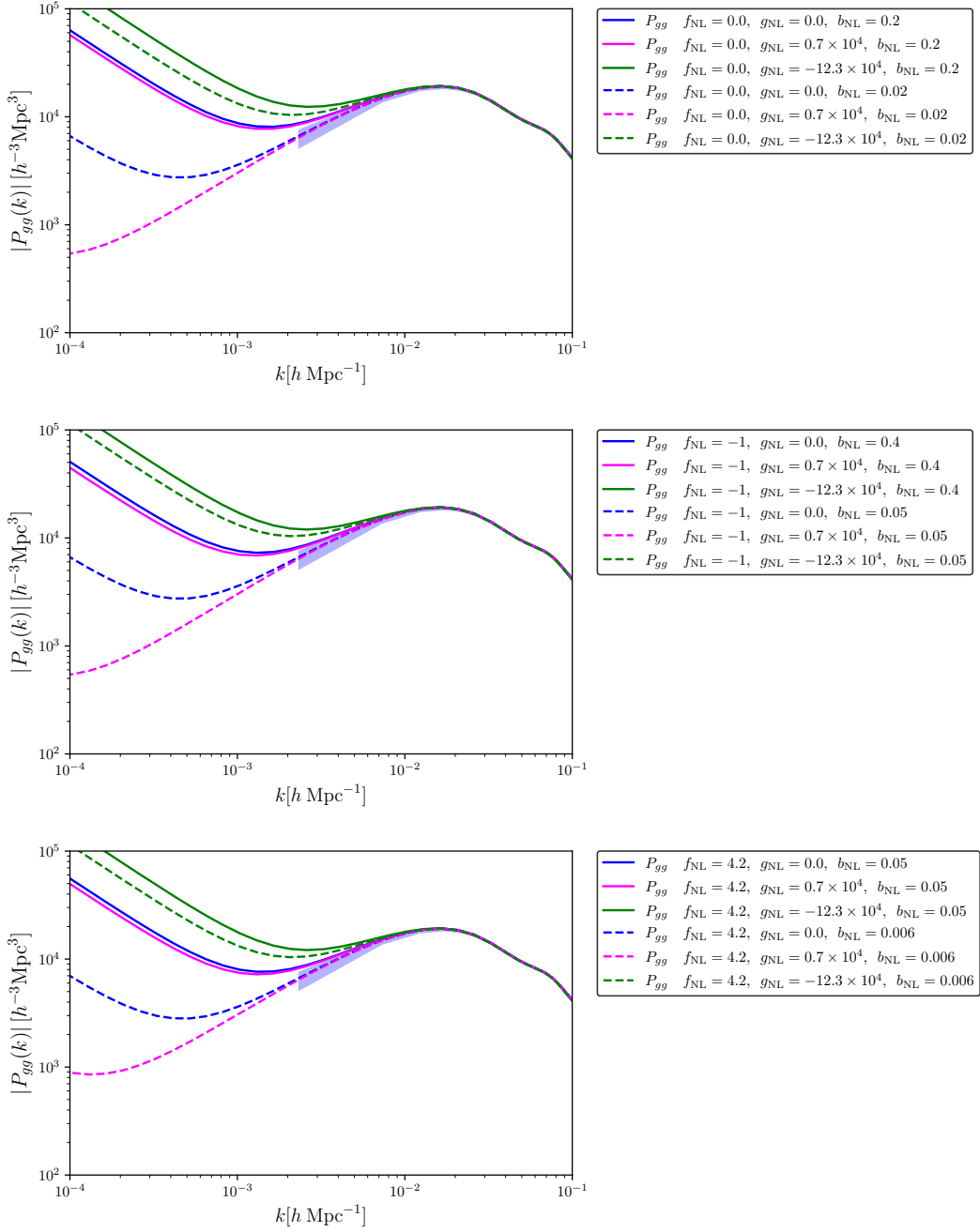


Figure 4: Galaxy power spectrum at redshift $z = 1$, with $b_\delta = 1.41$ (a choice justified in the text), for the limiting values of f_{NL} (zero for the top plot, -1 for the middle plot, and 4.2 for the bottom) each with limiting g_{NL} values reported by Planck [57]. The blue shaded area corresponds to the forecasted 1σ uncertainties of a cosmic variance limited survey of $40,000 \text{ deg}^2$. See text for more details.

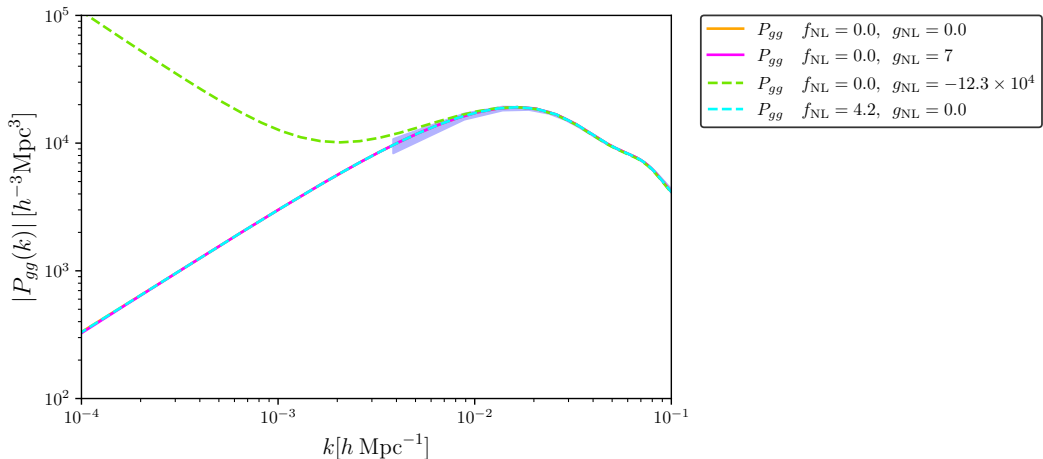


Figure 5: Renormalized galaxy power spectrum, at redshift $z = 1$, with the specific choice of $b_\delta = 1.41$, and $b_{\text{NL}} = 2.44 \times 10^{-6}$. The lines show limiting values of f_{NL} and g_{NL} as reported by Planck [57]. The shaded area is as described in Fig. 3. Note that only the largest g_{NL} value yields a distinguishable departure from the linear spectrum.

5 Discussion

In this paper we have computed the non-linear galaxy power spectrum including the leading order relativistic and primordial non-Gaussianity contributions, modulated through a set of bias parameters that follow closely the standard prescriptions.

Besides identifying the well known scale-dependent bias feature, we have non-linear contributions from the relativistic treatment of the matter density. The main result is the galaxy power spectrum including one-loop corrections, expressed in Eq. (3.10), with the different elements plotted and discussed in detail in section 4. In order to assess the detectability of such contributions, our plots include the predicted 1σ uncertainties of planned Stage-IV galaxy surveys, thus showing which parameter values may be discriminated in future galaxy catalogues. However, we note that we have not included contributions from redshift space distortions (see e.g. Ref. [11]). We leave this to future work.

An important first result is that, even in the absence of PNG, some values of the non-linear bias parameter could be discriminated by future surveys ($b_{\text{NL}} \gtrsim 0.3$), which, conversely means that relativistic contributions could be detected in the galaxy power spectrum. On the other hand, such signal is degenerate with that of a large f_{NL} since the scale-dependence is identical for relativistic and PNG terms at large scales (see e.g. Fig. 2).

The so-called universality relations between bias parameters would fix values of b_ϕ allowing to debias contributions of PNG parameters in the Newtonian formalism [14, 15, 60]. However, we find that the corresponding values for b_{NL} from the universality relation are larger than all the examples here of section 4.1. This calls for numerical simulations of galaxy formation and complementary probes of non-Gaussianity in the galaxy or lensing maps, in order to reanalyse the correspondence between bias parameters and also to disentangle relativistic and PNG contributions.

Alternatively, a suitable value of the non-linear bias parameter b_{NL} can be chosen in order to cancel the divergences of the different contributions at the largest scales, as we show in section 4.2. This represents an effective renormalization of the general relativistic

corrections to the galaxy power spectrum, so they remain convergent at all scales. In this case, and as shown in Fig. 5, the non-Gaussianity contributions can be distinguished from relativistic corrections.

It is important to note that an extreme value of the g_{NL} parameter, as allowed by Planck constraints, yields the maximum contribution of the non-linear terms to $P_{gg}(k, \eta)$, even when $b_{\text{NL}} = 0$. In such case, our plots show that values of order $g_{\text{NL}} \sim -10^5$ could be detected (or ruled out) in the planned all-sky surveys. We thus conclude that g_{NL} should not be ignored in the search for primordial non-Gaussianities imprinted in the galaxy power spectrum.

While our results do not account for the full relativistic effects in the observed galaxy distribution, we are confident to have at hand a tool for incorporating the dominant contributions from PNG and relativistic non-linearities into the theoretical galaxy power spectrum.

Acknowledgments

We thank Obinna Umeh for useful discussions. RMC acknowledges support of a studentship funded by Queen Mary University of London and CONACyT grant No. 661285. AP is a UK Research and Innovation Future Leaders Fellow, grant MR/S016066/1. JCH acknowledges sponsorship from CONACyT through grant CB-2016-282569, and FORDECYT-PRONACES project No. 304001/2020, as well as grant PAPIIT-UNAM IN107521 (*Sector Oscuro y Agujeros Negros Primordiales*). KAM is supported by STFC grants ST/P000592/1 and ST/T000341/1.

References

- [1] R. Laureijs, J. Amiaux, S. Arduini, J. L. Auguères, J. Brinchmann, R. Cole et al., *Euclid Definition Study Report, arXiv e-prints* (2011) arXiv:1110.3193 [[1110.3193](#)].
- [2] DESI Collaboration, A. Aghamousa, J. Aguilar, S. Ahlen, S. Alam, L. E. Allen et al., *The DESI Experiment Part I: Science, Targeting, and Survey Design, arXiv e-prints* (2016) arXiv:1611.00036 [[1611.00036](#)].
- [3] N. E. Chisari, D. Alonso, E. Krause, C. D. Leonard, P. Bull, J. Neveu et al., *Core Cosmology Library: Precision Cosmological Predictions for LSST, ApJS* **242** (2019) 2 [[1812.05995](#)].
- [4] C. Carbone, L. Verde and S. Matarrese, *Non-Gaussian Halo Bias and Future Galaxy Surveys, ApJL* **684** (2008) L1 [[0806.1950](#)].
- [5] A. Slosar, C. Hirata, U. Seljak, S. Ho and N. Padmanabhan, *Constraints on local primordial non-Gaussianity from large scale structure, JCAP* **2008** (2008) 031 [[0805.3580](#)].
- [6] N. Hamaus, U. Seljak and V. Desjacques, *Optimal constraints on local primordial non-Gaussianity from the two-point statistics of large-scale structure, Phys. Rev. D* **84** (2011) 083509 [[1104.2321](#)].
- [7] T. Giannantonio, C. Porciani, J. Carron, A. Amara and A. Pillepich, *Constraining primordial non-Gaussianity with future galaxy surveys, MNRAS* **422** (2012) 2854 [[1109.0958](#)].
- [8] A. J. Ross, W. J. Percival, A. Carnero, G.-b. Zhao, M. Manera, A. Raccanelli et al., *The clustering of galaxies in the SDSS-III DR9 Baryon Oscillation Spectroscopic Survey: constraints on primordial non-Gaussianity, MNRAS* **428** (2013) 1116 [[1208.1491](#)].
- [9] S. Ferraro and K. M. Smith, *Using large scale structure to measure f_{NL} , g_{NL} and τ_{NL} , Phys. Rev. D* **91** (2015) 043506 [[1408.3126](#)].
- [10] R. de Putter and O. Doré, *Designing an inflation galaxy survey: How to measure $\sigma(f_{\text{NL}}) \sim 1$ using scale-dependent galaxy bias, Phys. Rev. D* **95** (2017) 123513 [[1412.3854](#)].

- [11] D. Karagiannis, A. Lazanu, M. Liguori, A. Raccanelli, N. Bartolo and L. Verde, *Constraining primordial non-Gaussianity with bispectrum and power spectrum from upcoming optical and radio surveys*, *MNRAS* **478** (2018) 1341 [[1801.09280](#)].
- [12] E. Castorina, N. Hand, U. Seljak, F. Beutler, C.-H. Chuang, C. Zhao et al., *Redshift-weighted constraints on primordial non-Gaussianity from the clustering of the eBOSS DR14 quasars in Fourier space*, *JCAP* **2019** (2019) 010 [[1904.08859](#)].
- [13] D. Karagiannis, A. Slosar and M. Liguori, *Forecasts on primordial non-Gaussianity from 21 cm intensity mapping experiments*, *JCAP* **2020** (2020) 052 [[1911.03964](#)].
- [14] A. Barreira, *On the impact of galaxy bias uncertainties on primordial non-Gaussianity constraints*, *JCAP* **2020** (2020) 031 [[2009.06622](#)].
- [15] A. Barreira, *Predictions for local PNG bias in the galaxy power spectrum and bispectrum and the consequences for f_{NL} constraints*, *arXiv e-prints* (2021) arXiv:2107.06887 [[2107.06887](#)].
- [16] A. Pezzotta, M. Crocce, A. Eggemeier, A. G. Sánchez and R. Scoccimarro, *Testing one-loop galaxy bias: cosmological constraints from the power spectrum*, *arXiv e-prints* (2021) arXiv:2102.08315 [[2102.08315](#)].
- [17] N. Dalal, O. Doré, D. Huterer and A. Shirokov, *Imprints of primordial non-Gaussianities on large-scale structure: Scale-dependent bias and abundance of virialized objects*, *Phys. Rev. D* **77** (2008) 123514 [[0710.4560](#)].
- [18] T. Giannantonio and C. Porciani, *Structure formation from non-Gaussian initial conditions: Multivariate biasing, statistics, and comparison with N-body simulations*, *Phys. Rev. D* **81** (2010) 063530 [[0911.0017](#)].
- [19] R. Angulo, M. Fasiello, L. Senatore and Z. Vlah, *On the statistics of biased tracers in the Effective Field Theory of Large Scale Structures*, *JCAP* **2015** (2015) 029 [[1503.08826](#)].
- [20] V. Assassi, D. Baumann and F. Schmidt, *Galaxy bias and primordial non-Gaussianity*, *JCAP* **2015** (2015) 043 [[1510.03723](#)].
- [21] A. Eggemeier, R. Scoccimarro, M. Crocce, A. Pezzotta and A. G. Sánchez, *Testing one-loop galaxy bias: Power spectrum*, *Phys. Rev. D* **102** (2020) 103530 [[2006.09729](#)].
- [22] V. Desjacques, D. Jeong and F. Schmidt, *Large-scale galaxy bias*, *Phys. Rep.* **733** (2018) 1 [[1611.09787](#)].
- [23] J. Yoo, A. L. Fitzpatrick and M. Zaldarriaga, *New perspective on galaxy clustering as a cosmological probe: General relativistic effects*, *Phys. Rev. D* **80** (2009) 083514 [[0907.0707](#)].
- [24] J. Yoo, *General relativistic description of the observed galaxy power spectrum: Do we understand what we measure?*, *Phys. Rev. D* **82** (2010) 083508 [[1009.3021](#)].
- [25] A. Challinor and A. Lewis, *Linear power spectrum of observed source number counts*, *Phys. Rev. D* **84** (2011) 043516 [[1105.5292](#)].
- [26] C. Bonvin and R. Durrer, *What galaxy surveys really measure*, *Phys. Rev. D* **84** (2011) 063505 [[1105.5280](#)].
- [27] D. Jeong, F. Schmidt and C. M. Hirata, *Large-scale clustering of galaxies in general relativity*, *Phys. Rev. D* **85** (2012) 023504 [[1107.5427](#)].
- [28] J. Yoo, *Proper-time hypersurface of nonrelativistic matter flows: Galaxy bias in general relativity*, *Phys. Rev. D* **90** (2014) 123507 [[1408.5137](#)].
- [29] J. L. Fuentes, J. C. Hidalgo and K. A. Malik, *Galaxy number counts at second order: an independent approach*, *arXiv e-prints* (2019) arXiv:1908.08400 [[1908.08400](#)].
- [30] J. L. Fuentes, J. C. Hidalgo and K. A. Malik, *Galaxy number counts at second order in perturbation theory: a leading-order term comparison*, *arXiv e-prints* (2020) arXiv:2012.15326 [[2012.15326](#)].

- [31] T. Baldauf, U. Seljak, L. Senatore and M. Zaldarriaga, *Galaxy bias and non-linear structure formation in general relativity*, *JCAP* **2011** (2011) 031 [[1106.5507](#)].
- [32] N. Bartolo, S. Matarrese and A. Riotto, *Relativistic effects and primordial non-Gaussianity in the galaxy bias*, *JCAP* **2011** (2011) 011 [[1011.4374](#)].
- [33] M. Bruni, R. Crittenden, K. Koyama, R. Maartens, C. Pitrou and D. Wands, *Disentangling non-Gaussianity, bias, and general relativistic effects in the galaxy distribution*, *Phys. Rev. D* **85** (2012) 041301 [[1106.3999](#)].
- [34] O. Umeh, K. Koyama, R. Maartens, F. Schmidt and C. Clarkson, *General relativistic effects in the galaxy bias at second order*, *JCAP* **2019** (2019) 020 [[1901.07460](#)].
- [35] O. Umeh and K. Koyama, *The galaxy bias at second order in general relativity with non-Gaussian initial conditions*, *JCAP* **2019** (2019) 048 [[1907.08094](#)].
- [36] L. Castiblanco, R. Gannouji, J. Noreña and C. Stahl, *Relativistic cosmological large scale structures at one-loop*, *JCAP* **2019** (2019) 030 [[1811.05452](#)].
- [37] J. Calles, L. Castiblanco, J. Noreña and C. Stahl, *From matter to galaxies: General relativistic bias for the one-loop bispectrum*, *arXiv e-prints* (2019) arXiv:1912.13034 [[1912.13034](#)].
- [38] N. Grimm, F. Scaccabarozzi, J. Yoo, S. G. Biern and J.-O. Gong, *Galaxy power spectrum in general relativity*, *JCAP* **2020** (2020) 064 [[2005.06484](#)].
- [39] E. Castorina and E. di Dio, *The observed galaxy power spectrum in General Relativity*, *arXiv e-prints* (2021) arXiv:2106.08857 [[2106.08857](#)].
- [40] R. Martinez-Carrillo, J. De-Santiago, J. C. Hidalgo and K. A. Malik, *Relativistic and non-Gaussianity contributions to the one-loop power spectrum*, *JCAP* **2020** (2020) 028 [[1911.04359](#)].
- [41] P. McDonald, *Clustering of dark matter tracers: Renormalizing the bias parameters*, *Phys. Rev. D* **74** (2006) 103512 [[astro-ph/0609413](#)].
- [42] P. McDonald, *Primordial non-Gaussianity: Large-scale structure signature in the perturbative bias model*, *Phys. Rev. D* **78** (2008) 123519 [[0806.1061](#)].
- [43] D. Bertacca, N. Bartolo, M. Bruni, K. Koyama, R. Maartens, S. Matarrese et al., *Galaxy bias and gauges at second order in general relativity*, *Classical and Quantum Gravity* **32** (2015) 175019 [[1501.03163](#)].
- [44] H. A. Gressel and M. Bruni, *f_{NL} - g_{NL} mixing in the matter density field at higher orders*, *JCAP* **2018** (2018) 016 [[1712.08687](#)].
- [45] M. Bruni, J. C. Hidalgo, N. Meures and D. Wands, *Non-Gaussian Initial Conditions in Λ CDM: Newtonian, Relativistic, and Primordial Contributions*, *ApJ* **785** (2014) 2 [[1307.1478](#)].
- [46] M. Bruni, J. C. Hidalgo and D. Wands, *Einstein's Signature in Cosmological Large-scale Structure*, *ApJL* **794** (2014) L11 [[1405.7006](#)].
- [47] K. A. Malik and D. Wands, *Cosmological perturbations*, *Phys. Rep.* **475** (2009) 1 [[0809.4944](#)].
- [48] K. A. Malik and D. R. Matravers, *TOPICAL REVIEW: A concise introduction to perturbation theory in cosmology*, *Classical and Quantum Gravity* **25** (2008) 193001 [[0804.3276](#)].
- [49] N. Meures, *General Relativistic Effects on Cosmological Observations*, Ph.D. thesis, University of Portsmouth, 2012.
- [50] D. S. Salopek and J. R. Bond, *Nonlinear evolution of long-wavelength metric fluctuations in inflationary models*, *Phys. Rev. D* **42** (1990) 3936.
- [51] D. H. Lyth, K. A. Malik and M. Sasaki, *A general proof of the conservation of the curvature perturbation*, *JCAP* **2005** (2005) 004 [[astro-ph/0411220](#)].

- [52] D. Wands, *Local non-Gaussianity from inflation*, *Classical and Quantum Gravity* **27** (2010) 124002 [[1004.0818](#)].
- [53] J. Lesgourgues, *The Cosmic Linear Anisotropy Solving System (CLASS) I: Overview*, *arXiv e-prints* (2011) arXiv:1104.2932 [[1104.2932](#)].
- [54] D. Blas, J. Lesgourgues and T. Tram, *The Cosmic Linear Anisotropy Solving System (CLASS). Part II: Approximation schemes*, *JCAP* **2011** (2011) 034 [[1104.2933](#)].
- [55] Planck Collaboration, P. A. R. Ade, N. Aghanim, M. Arnaud, M. Ashdown, J. Aumont et al., *Planck 2015 results. XIII. Cosmological parameters*, *A&A* **594** (2016) A13 [[1502.01589](#)].
- [56] Euclid Collaboration, A. Blanchard, S. Camera, C. Carbone, V. F. Cardone, S. Casas et al., *Euclid preparation. VII. Forecast validation for Euclid cosmological probes*, *A&A* **642** (2020) A191 [[1910.09273](#)].
- [57] Planck Collaboration, Y. Akrami, F. Arroja, M. Ashdown, J. Aumont, C. Baccigalupi et al., *Planck 2018 results. IX. Constraints on primordial non-Gaussianity*, *A&A* **641** (2020) A9 [[1905.05697](#)].
- [58] M. Tegmark, *Measuring Cosmological Parameters with Galaxy Surveys*, *Phys. Rev. Lett.* **79** (1997) 3806 [[astro-ph/9706198](#)].
- [59] E.-M. Mueller, M. Rezaie, W. J. Percival, A. J. Ross, R. Ruggeri, H.-J. Seo et al., *The clustering of galaxies in the completed SDSS-IV extended Baryon Oscillation Spectroscopic Survey: Primordial non-Gaussianity in Fourier Space*, *arXiv e-prints* (2021) arXiv:2106.13725 [[2106.13725](#)].
- [60] M. Martinelli, R. Dalal, F. Majidi, Y. Akrami, S. Camera and E. Sellentin, *Ultra-large-scale approximations and galaxy clustering: debiasing constraints on cosmological parameters*, *arXiv e-prints* (2021) arXiv:2106.15604 [[2106.15604](#)].